



اویونسیتی تیکنیکال ملیسیا ملاک

UNIVERSITI TEKNIKAL MALAYSIA MELAKA

## STREAMING IN OSCILLATORY FLOW THROUGH POROUS CHANNELS IN THERMOACOUSTICS

NUR AFIQAH AINA BINTI ZAIHAM

UNIVERSITI TEKNIKAL MALAYSIA MELAKA

MASTER OF SCIENCE IN MECHANICAL ENGINEERING

2025



اونیورسیتی تکنیکال ملیسیا ملاک

UNIVERSITI TEKNIKAL MALAYSIA MELAKA

## Faculty of Mechanical Technology and Engineering

STREAMING IN OSCILLATORY FLOW THROUGH POROUS  
CHANNELS IN THERMOACOUSTICS

Nur Afiqah Aina Binti Zaiham

اونیورسیتی تکنیکال ملیسیا ملاک

UNIVERSITI TEKNIKAL MALAYSIA MELAKA

Master of Science in Mechanical Engineering

2025

**STREAMING IN OSCILLATORY FLOW THROUGH POROUS CHANNELS IN  
THERMOACOUSTICS**

**NUR AFIQAH AINA BINTI ZAIHAM**



**A thesis submitted in fulfillment of the requirements for the degree of  
Master of Science in Mechanical Engineering**

**جامعة ملاكا التقنية**

**UNIVERSITI TEKNIKAL MALAYSIA MELAKA**

**UNIVERSITI TEKNIKAL MALAYSIA MELAKA**

**2025**

## DECLARATION

I declare that this thesis entitled “Streaming in Oscillatory Flow Through Porous Channels in Thermoacoustics” is the result of my own research except as cited in the references. The thesis has not been accepted for any degree and is not concurrently submitted in candidature of any other degree.



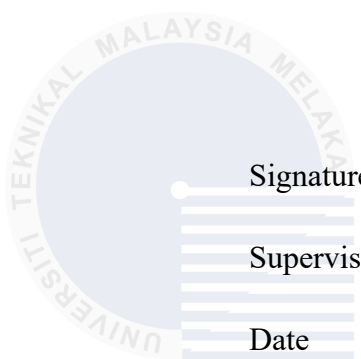
Signature : .....  
Name : NUR AFIQAH AINA BINTI ZAIHAM  
Date : 09 SEPTEMBER 2025

جامعة ملاكا التقنية

UNIVERSITI TEKNIKAL MALAYSIA MELAKA

## APPROVAL

I hereby declare that I have read this thesis and in my opinion this thesis is sufficient in terms of scope and quality for the award of Master of Science in Mechanical Engineering



Signature

: .....

Supervisor Name

: FATIMAH AL-ZAHRAH BINTI MOHD SA'AT

Date

: 09 SEPTEMBER 2025

جامعة ملaka التقنية

UNIVERSITI TEKNIKAL MALAYSIA MELAKA

## DEDICATION

I dedicate this work to my parents, who taught me the value of perseverance, to my loved one, who has been my constant source of strength and to my friends, who never stopped believing in me.



اویونسیتی تکنیکال ملیسیا ملاک

---

UNIVERSITI TEKNIKAL MALAYSIA MELAKA

## ABSTRACT

Streaming in oscillatory flow of the alternative green technology known as thermoacoustics remains relatively less understood. The thermodynamic cycle in the system is driven by the oscillatory flow of the acoustic waves, understanding the nature of streaming, particularly within the porous structure of the system is crucial. Since the current study does not include a heat exchanger to generate a temperature gradient, it cannot directly be used as a complete thermoacoustic system. Instead, this design choice aligns with the primary aim of the study, which was to investigate the flow dynamics and acoustic streaming within an oscillatory flow field in a thermoacoustic system without thermal effect. This study was done using a parallel-plate porous channel operating under standing-wave conditions at a quarter wavelength. Both experimental and computational fluid dynamics (CFD) approaches were used. The experimental data, including the velocity, pressure and wall displacement were recorded under a resonance frequency of 23.6 Hz. The flow was maintained at room temperature and atmospheric pressure, with drive ratios ranging from 0.64% to 3.01%. These measurements were then incorporated into CFD simulations to provide deeper insight into complex flow physics. The two-dimensional (2D) CFD model was solved for minimum, medium and maximum flow conditions using the Shear Stress Transport (SST)  $k-\omega$  turbulence model. Comparisons and discussions were made based on the data from the experiment, CFD and one-dimensional linear thermoacoustic theory. Results showed that the discrepancies between experimental and numerical results were slightly larger, possibly due to vibration effects during testing. To address this, a dynamic mesh was applied to simulate wall movement. This adjustment results in a slightly improved correlation with experimental data, especially for peak velocity at the downstream location. Further analysis of vortex structures over 20 phases of a flow cycle was carried out. The results show that under moving wall conditions, vortices shed further and extended longer into the open area, with a 12.40% deviation from the non-moving wall case at high acoustic amplitudes. The observation of flow streaming was made based on the progress of velocity profiles over time. In addition, the CFD model was extended with the Ffowcs-Williams and Hawkings (FW-H) acoustic model to analyse the sound pressure level (SPL) at three receivers positioned at the inlet, mid-channel and outlet of the computational domain. The highest SPL was recorded at the mid-channel, attributed to strong interactions between acoustic waves and solid boundaries, with the acoustic source positioned at the inlet. A parametric study using helium as the working fluid was also conducted to explore the effect of fluid properties on flow behavior and streaming. The simulations were conducted under the same drive ratios as those used for air. Results showed that Rayleigh streaming in helium is significantly weaker than in air, with a reduction in streaming intensity of approximately 34.17%, while Schlichting streaming appeared negligible. These findings were further strengthened by comparisons with existing literature, reinforcing the validity of the proposed methodology. Overall, this study provides new insights into nonlinear flow behavior in thermoacoustics. The findings enhance predictive modelling of oscillatory flows in porous channels and support the design of more efficient thermoacoustic systems for sustainable cooling, waste-heat recovery and renewable energy conversion.

## **PENJURUSAN DALAM ALIRAN AYUNAN MELALUI SALURAN BERLIANG DALAM TERMOAKUSTIK**

### **ABSTRAK**

*Penjurusan dalam aliran ayunan bagi teknologi hijau alternatif termoakustik masih kurang difahami. Sistem ini dipacu oleh aliran ayunan gelombang akustik, maka pemahaman terhadap sifat penjurusan, khususnya berhampiran struktur berliang, amat penting untuk memastikan prestasi optimum. Kajian ini tidak melibatkan penukar haba untuk menjana kecerunan suhu, oleh itu ia bukan sistem termoakustik lengkap, sebaliknya menumpukan pada penyelidikan dinamik aliran dan penjurusan akustik tanpa kesan haba. Kajian dijalankan menggunakan saluran berliang plat selari yang beroperasi di bawah gelombang pegun dengan konfigurasi suku panjang gelombang. Pendekatan eksperimen dan CFD digunakan, di mana data halaju aliran, tekanan dan pergerakan dinding direkodkan pada frekuensi resonan 23.6 Hz dalam keadaan suhu bilik dan tekanan atmosfera, dengan julat nisbah pacuan 0.64%–3.01%. Data ini seterusnya digunakan dalam simulasi CFD untuk memahami tingkah laku fizikal aliran yang kompleks. Model CFD dua dimensi (2D) diselesaikan bagi keadaan aliran minimum, sederhana dan maksimum menggunakan model pergolakan SST  $k-\omega$ . Perbandingan dibuat dengan data eksperimen dan teori linear satu dimensi. Hasil menunjukkan terdapat sedikit perbezaan antara eksperimen dan simulasi yang berkemungkinan disebabkan oleh kesan getaran. Bagi menangani isu ini, jejaring dinamik digunakan untuk mensimulasikan pergerakan dinding, menghasilkan korelasi lebih baik dengan data eksperimen, khususnya pada halaju puncak di lokasi hujung. Analisis pusaran bagi 20 fasa kitaran aliran mendapati dinding bergerak menghasilkan pusaran yang memanjang 12.40% lebih jauh ke arah kawasan terbuka berbanding kes dinding statik pada amplitud tinggi. Model CFD turut diperluas dengan model akustik Ffowcs-Williams dan Hawkings (FW-H) untuk menganalisis tahap tekanan bunyi (SPL) pada penerima di bahagian masuk, tengah dan keluar saluran. SPL tertinggi diperoleh di bahagian tengah saluran, disebabkan interaksi kuat antara gelombang akustik dan dinding pepejal, dengan sumber akustik terletak di bahagian masuk. Selain itu, kajian parametrik menggunakan helium sebagai bendalir kerja dijalankan bagi menilai kesan sifat bendalir. Simulasi dengan nisbah pacuan yang sama seperti udara menunjukkan penjurusan Rayleigh dalam helium jauh lebih lemah, dengan pengurangan sekitar 34.17%, manakala penjurusan Schlichting hampir tiada. Penemuan ini konsisten dengan kajian terdahulu, sekali gus mengesahkan pendekatan kajian. Secara keseluruhan, kajian ini memberikan pandangan baharu mengenai tingkah laku aliran bukan linear dalam termoakustik, meningkatkan pemodelan ramalan aliran ayunan dalam saluran berliang serta menyokong pembangunan sistem termoakustik yang lebih cekap untuk penyejukan mampan, pemulihan haba buangan dan penukaran tenaga boleh diperbaharui.*

## **ACKNOWLEDGEMENT**

In the Name of Allah, the Most Gracious, the Most Merciful. First and foremost, I would like to take this opportunity to express my sincere acknowledgement to all who have supported me throughout the course of this research and the completion of this thesis.

Firstly, I would like to express my heartfelt gratitude to my supervisor, Dr. Fatimah Al-Zahrah binti Mohd Sa‘at and my co-supervisor, Dr. Fadhilah binti Shikh Anuar for their invaluable guidance, patience, and continuous support throughout the course of this research and the completion of this thesis.

I would also like to extend my sincere appreciation to the technicians and laboratory assistants, particularly Mr. Faizal bin Jaafar for his kind assistance, technical advice and support during the experimental phase of this study.

Special thanks are also due to the Ministry of Higher Education Malaysia for the financial support provided under the research grant FRGS/1/2023/TK08/UTEM/02/1 and to Universiti Teknikal Malaysia Melaka (UTeM) for the opportunity and facilities provided to carry out this research work.

Lastly, from the bottom of my heart, I want to thank my beloved family, my dearest loved one and my supportive friends for always standing by me with endless patience, encouragement and love. Your support has carried me through the hardest moments of this journey. To everyone who has, in any way, contributed to the successful realization of this project, I extend my sincere appreciation and heartfelt thanks.

## TABLE OF CONTENTS

	<b>PAGES</b>
<b>DECLARATION</b>	<b>i</b>
<b>APPROVAL</b>	<b>ii</b>
<b>DEDICATION</b>	<b>iii</b>
<b>ABSTRACT</b>	<b>iv</b>
<b>ABSTRAK</b>	<b>vii</b>
<b>ACKNOWLEDGEMENT</b>	<b>ix</b>
<b>TABLE OF CONTENTS</b>	<b>xiii</b>
<b>LIST OF TABLES</b>	<b>xiv</b>
<b>LIST OF FIGURES</b>	<b>xvi</b>
<b>LIST OF ABBREVIATIONS</b>	
<b>LIST OF SYMBOLS</b>	
<b>LIST OF PUBLICATIONS</b>	
 <b>CHAPTER</b>	
<b>1. INTRODUCTION</b>	<b>1</b>
1.1 Background	1
1.2 Problem Statement	6
1.3 Research Objectives	8
1.4 Scope of Research	8
1.5 Significance of the Study	10
1.6 Thesis Outline	10
<b>2. LITERATURE REVIEW</b>	<b>12</b>
2.1 Thermoacoustic System	12
2.1.1 Types of Thermoacoustic System	14
2.1.2 Thermoacoustic cycle	16
2.1.3 Types of Waves in Thermoacoustic System	19
2.2 Operating Condition in Thermoacoustic System	22
2.2.1 Pressure amplitude	22
2.2.2 Operating Frequency	25
2.2.3 Working Fluid	27
2.3 Basic Components of Thermoacoustic System	31
2.3.1 Resonator	32
2.3.2 Porous as Stack	36
2.3.3 Acoustic Driver	41
2.4 Fluid Flow in Thermoacoustic System	42
2.4.1 Oscillatory Flow	43
2.4.2 Streaming in Flow	45
2.5 Vibration in Thermoacoustic System	47
2.6 Acoustic Modelling	49
2.7 Numerical Investigation	51
2.7.1 Computational Fluid Dynamics (CFD)	51
2.7.2 Meshing geometry	53
2.7.3 Governing Equation	55

2.8	Flow Investigation in Thermoacoustic	58
2.8.1	Velocity Behavior	58
2.8.2	Vortex Pattern	60
2.9	Summary of the Chapter	62
<b>3.</b>	<b>METHODOLOGY</b>	<b>66</b>
3.1	General Methodology	66
3.2	Experimental Work	70
3.2.1	Experimental Setup	70
3.2.2	Calibration of Thermoacoustic Test Rig	76
3.2.3	Data Collection	77
3.2.4	Verification of Experimental Data	79
3.2.5	Data Reduction and Uncertainty	81
3.3	Numerical Analysis	83
3.3.1	Modelling CFD Geometry	83
3.3.2	Mesning Geometry	85
3.3.3	Boundary and Fluid Condition Setting	87
3.3.4	Solver Setting	92
3.3.5	Grid Independency Test	98
3.3.6	Solving and Validation of Model	99
3.3.7	Parametric Investigation of Different Working Fluid	103
3.3.8	Data analysis	104
3.4	Limitations of the Study	105
3.5	Summary of the Chapter	106
<b>4.</b>	<b>RESULT AND DISCUSSION</b>	<b>108</b>
4.1	Experimental Results	108
4.1.1	Resonance Test	108
4.1.2	Validation of Experimental Data	110
4.1.3	Velocity at the Upstream and Downstream Location	113
4.1.4	Vibration of the Resonator Wall	115
4.2	Numerical Results	119
4.2.1	Grid Independency Test	119
4.2.2	Validation of CFD Model	121
4.2.3	Analysis of CFD for Moving and Non-Moving Wall Cases	124
4.2.4	Validation of Moving Wall Case	127
4.3	Vortex Structure Analysis	129
4.4	Streaming in Thermoacoustic	140
4.4.1	Rayleigh Streaming	143
4.4.2	Schlichting Streaming	149
4.5	Comparison of Results with Existing Literature	157
4.6	Helium as a Working Fluid	160
4.6.1	Validation of helium model	161
4.6.2	Comparison Between Air and Helium on Velocity Result	162
4.6.3	Comparison Between Air and Helium on Vortex Contour	164
4.6.4	Comparison Between Moving and Non-Moving Wall Cases	168
4.6.5	Streaming in Helium Model	169

4.7	Analysis of SPL within the Thermoacoustic System	173
4.7.1	Comparison of the SPL at Three Acoustic Receivers	174
4.7.2	Comparison of the SPL Using Air and Helium as the Working Fluid	176
4.7.3	Comparison of the SPL with Existing Literature	180
4.8	Summary of the Chapter	181
<b>5.</b>	<b>CONCLUSION AND RECOMMENDATIONS FOR FUTURE RESEARCH</b>	<b>182</b>
5.1	Conclusion	182
5.2	Contributions of Study	183
5.3	Limitations and Recommendations for Future Works	184
<b>REFERENCES</b>		<b>185</b>



## LIST OF TABLES

TABLE	TITLE	PAGE
Table 2.1	Fluid properties of the ideal noble gases at standard conditions (298 K, 1 atm) (Belcher et al., 1999; Yang et al., 2010; Vesely and Vit, 2014)	30
Table 2.2	Acoustic modelling in thermoacoustic system for existing literature	50
Table 2.3	Velocity amplitude data at different drive ratios for two operating frequencies Almukhtar Allaifi and Mohd Saat (2022)	60
Table 2.4	Summary of previous study related to vibration in thermoacoustic systems	64
Table 3.1	Detail descriptions of components and measurement devices	76
Table 3.2	Mesh quality	86
Table 3.3	Boundary conditions of geometry model	89
Table 3.4	Fluid and material properties	90
Table 3.5	Under-relaxation values for solver setting	95
Table 3.6	Residual convergence conditions	96
Table 3.7	Points created in CFD domain	97
Table 3.8	Mesh numbers for grid independency test	99
Table 3.9	Properties of Helium	104
Table 4.1	Velocity amplitude at the downstream location of resonator for oscillatory flow conditions	127
Table 4.2	Vortex structure elongation at the end of the plate for moving and non-moving walls case	140
Table 4.3	Vortex structures of the oscillating flow model over time at a drive ratio of 3.01% for $\varnothing 5$	142
Table 4.4	Conditions of existing literature and current study	159

Table 4.5	Comparison of vortex structure between air and helium at drive ratio of 0.64%	165
Table 4.6	Comparison of vortex structure between air and helium at drive ratio of 2.17%	166
Table 4.7	Comparison of vortex structure between air and helium at drive ratio of 3.01%	167
Table 4.8	Comparison of vortex structures between non-moving and moving wall cases at $\varnothing 5$ across different drive ratios	168
Table 4.9	Condition of SPL at different locations	176
Table 4.10	Condition of SPL for air and helium at receiver 2	179
Table 4.11	Comparison of SPL value between existing literature and current study	181

جامعة ملاكا  
UNIVERSITI TEKNIKAL MALAYSIA MELAKA

## LIST OF FIGURES

FIGURE	TITLE	PAGE
Figure 1.1	Simple schematic diagram of the thermoacoustic refrigerator Kajurek and Rusowic (2021)	3
Figure 2.1	The principle of the (a) thermoacoustic engine and (b) thermoacoustic refrigerator (Novotny et al. 2012)	15
Figure 2.2	Schematic diagram of combine thermoacoustic engine and thermoacoustic refrigerator (Ali et al. 2023)	16
Figure 2.3	Schematic diagram of (a) conventional heat engine and (b) thermoacoustic engine	18
Figure 2.4	Schematic diagram of (a) vapor-compression refrigerator and (b) thermoacoustic refrigerator	19
Figure 2.5	Time phasing between pressure and velocity inside (a) standing wave (b) travelling wave system (Mohd Saat 2013)	20
Figure 2.6	Half-wavelength and quarter-wavelength thermoacoustic system with pressure nodes and antinodes (Mumith et al. 2014)	23
Figure 2.7	Resonance frequency for the (a) 6.6 m long and (b) 3.8m long resonator (Mohd Saat et al. 2019a)	27
Figure 2.8	Schematic diagram of thermoacoustic refrigeration system (Kumar Sahu et al. 2022)	32
Figure 2.9	Schematic diagram of (a) straight resonator and (b) looped resonator (Chen et al. 2021)	33
Figure 2.10	A quarter-wavelenth resonator tube with spherical bulb at the closed end Bouramdane and Bah (2024)	35
Figure 2.11	Stack arrangement (a) spiral stack, (b) parallel plate, (c) honeycomb, (d) corning celcor and (e) pin array (Kumar Sahu et al. 2022)	37
Figure 2.12	Illustration of the region $\delta k$ , $\delta v$ and $\delta s$ within the stack channel (Amirin et al. 2019)	39
Figure 2.13	Position of stack between velocity and pressure node (Bagus and Hendradjit 2015)	40

Figure 2.14	Schematic diagram of flow direction (a) unidirectional flow and (b) bi-directional flow	43
Figure 2.15	Illustration of an oscillatory flow of a gas particle in thermoacoustic refrigeration cycle (Dyatmika et al. 2016)	44
Figure 2.16	Illustration of outer and inner acoustic streaming patterns (Meng et al. 2019)	46
Figure 2.17	An illustration of (a) structured mesh and (b) unstructured mesh (Thompson and Thompson 2017)	54
Figure 2.18	Skewness and orthogonality mesh quality metrics in ANSYS (Adam et al. 2020)	55
Figure 2.19	Illustration of pressure and velocity distribution inside resonator (Kajurek and Rusowicz 2018)	59
Figure 2.20	Formation of primary and secondary vortices at stack plate ends under oscillatory flow Mustaffa et al. (2018)	62
Figure 3.1	Flowchart of methodology	69
Figure 3.2	Actual picture of experimental setup	73
Figure 3.3	Schematic diagram of experimental setup	75
Figure 3.4	Component and measurement devices involved in experimental setup	75
Figure 3.5	2D geometry model	84
Figure 3.6	(a) Mesh generation of whole computational domain and (b) an enlarge view of mesh generation near parallel plate area	86
Figure 3.7	(a) Pressure and velocity changes along the quarter-wavelength resonator tube and (b) the velocity distribution for all 20 phases within one complete flow cycle	102
Figure 4.1	Resonance frequency test of 3.8 m long resonator	109
Figure 4.2	Validation of experimental velocity data against theoretical calculations at $x = 2.87$ m from the pressure antinode	111
Figure 4.3	Validation of experimental pressure data against theoretical calculations at different drive ratios	113

Figure 4.4	Comparison of velocity data at $x_1$ and $x_2$ from the pressure antinode	114
Figure 4.5	Vibration data along the x and y axes of the resonator at (a) $x_1$ and (b) $x_2$ from the pressure antinode	117
Figure 4.6	Comparison of vibration data at $x_1$ and $x_2$ along the Y-axis	118
Figure 4.7	Grid independence test for output velocity with varying grid refinement	120
Figure 4.8	Comparison of velocity data using CFD, experimental and theoretical approaches at different drive ratios	122
Figure 4.9	Comparison of CFD velocity output and the theoretical predictions across the one complete cycle at drive ratios of (a) 0.64%, (b) 2.17% and (c) 3.01%	123
Figure 4.10	Comparison of moving and non-moving wall cases across the one complete cycle at drive ratios of (a) 0.64%, (b) 2.17% and (c) 3.01%	126
Figure 4.11	Validation of moving wall data against experimental and non-moving wall data at different drive ratios	128
Figure 4.12	Vortex structure of non-moving wall case at drive ratio of 0.64%	131
Figure 4.13	Vortex structure of moving wall case at drive ratio of 0.64%	132
Figure 4.14	Vortex structure of non-moving wall case at drive ratio of 2.17%	134
Figure 4.15	Vortex structure of moving wall case at drive ratio of 2.17%	135
Figure 4.16	Vortex structure of non-moving wall case at drive ratio of 3.01%	137
Figure 4.17	Vortex structure of moving wall case at drive ratio of 3.01%	138
Figure 4.18	Five oscillation cycles with the representation of time at the peak of flow velocity	141
Figure 4.19	Locations of R1, R2 and R3 plot at the extremities of the model	143
Figure 4.20	Velocity profile of the oscillating flow model at location (a) R1, (b) R2 and (c) R3 at drive ratio of 0.64%	145
Figure 4.21	Velocity profile of the oscillating flow model for drive ratio of (a) 0.64%, (b) 2.17% and (c) 3.01% at location R2	147

Figure 4.22	Locations of S1, S2 and S3 plot along the channel of the middle plate	149
Figure 4.23	Velocity profile within the channel for a drive ratio of 0.64% at location (a) S1, (b) S2 and (c) S3	151
Figure 4.24	Velocity profile within the channel for a drive ratio of 2.17% at location (a) S1, (b) S2 and (c) S3	153
Figure 4.25	Velocity profile within the channel for a drive ratio of 3.01% at location (a) S1, (b) S2 and (c) S3	155
Figure 4.26	Comparison of dimensionless velocity data between the current study and existing literature for the CFD model	158
Figure 4.27	Validation of CFD model for helium case against theoretical calculations at different drive ratio	162
Figure 4.28	Comparison of velocity between air and helium for (a) non-moving wall and (b) moving wall cases at different drive ratios	164
Figure 4.29	Velocity profile of the helium model at location R2 for a peak condition at a drive ratio of 3.01% as time progresses from one cycle to another	170
Figure 4.30	Velocity profile of the helium model in the channel of the middle plate at a peak condition for a drive ratio of 3.01% at location (a) S1, (b) S2 and (c) S3 as time progresses from once cycle to another	172
Figure 4.31	Comparison of SPL at (a) receiver 1, (b) receiver 2 and (c) receiver 3	175
Figure 4.32	Comparison of SPL for (a) air and (b) helium at receiver 2	178

## LIST OF ABBREVIATIONS

CFC	-	chlorofluorocarbon
CFD	-	Computational fluid dynamics
DC	-	Direct current
FDM	-	Finite Difference Method
FEM	-	Finite Element Method
FFT	-	Fast Fourier Transform
FVM	-	Finite Volume Method
FW-H	-	Ffowcs-Williams and Hawking
HFC	-	hydrofluorocarbon
PISO	-	Pressure-Implicit with Splitting Operators
PIV	-	Particle Image Velocimetry
RANS	-	Reynolds Averaged Navier-Stokes
SPL	-	Sound pressure level
SST	-	Shear Stress Transport
UDF	-	User Defined Function
VCR	-	vapor-compression refrigeration

## LIST OF SYMBOLS

2D - two-dimensional

3D - three-dimensional

$c$  - Speed of sound

$P$  - pressure

$\rho$  - density

$F_R$  - resonant frequency

$L$  - length of resonator

$T$  - absolute temperature

$R$  - gas constant

$\gamma$  - Adiabatic gas constant

$Pr$  - Prandtl number

$\nu$  - kinematic viscosity

$\alpha$  - thermal diffusivity

$C_p$  - specific heat

$\mu$  - dynamic viscosity

$k$  - thermal conductivity

$\omega$  - angular frequency

$y_0$  - Plate spacing

$\delta v$  - viscous penetration depth

$\delta k$  - thermal penetration depth

$\lambda$  - wavelength

dB - decibels

Hz	-	Hertz
$k-\epsilon$	-	k-epsilon
$k-\omega$	-	k-omega
V <sub>pp</sub>	-	peak-to-peak voltage
d	-	thickness
D	-	Plate spacing
D	-	Tube diameter
v	-	velocity
DR	-	Drive ratio
Pa	-	Pascals
P <sub>m</sub>	-	mean pressure
$\dot{m}$	-	mass flow rate
$m'$	-	mass flux
$k_w$	-	wave number

UNIVERSITI TEKNOLOGAL MALAYSIA MELAKA

$\Delta$	-	Wall displacement
$\theta$	-	phase angle
$\phi$	-	Phase of cycle
I	-	turbulent intensity
l	-	turbulent length
$d_h$	-	hydraulic diameter
$P_{RMS}$	-	root mean square
S(x)	-	Swirling vector

## LIST OF PUBLICATIONS

The following is the publication related to the work presented in this thesis:

Zaiham, N. A. A., Saat, F. A. Z. M., Xuan, Y. Y., Anuar, F. S. and Saechan, P., 2024. The Effect of Vibration on Flow Inside a Standing Wave Thermoacoustic Condition. *International Journal of Integrated Engineering*, 16 (2), pp. 348–362.



# CHAPTER 1

## INTRODUCTION

This chapter introduces a brief background of the study focusing on the streaming phenomenon in oscillatory flow within thermoacoustic devices. The problem statement, research objectives and scope of the study are also explained.

### 1.1 Background

Pollution and global warming threats should no longer be taken lightly. Addressing these worldwide environmental issues is one of the most serious challenges for society in the twenty-first century (Laine et al. 2023). The energy supply sector is primarily responsible for the excessive use of fossil fuels, resulting in the release of significant amounts of greenhouse gases. This emission further leads to the release of unused waste heat, worsening the current global energy crisis and disrupting the fragile ecological balance (Chen et al. 2023). Given the worsening concern surrounding these matters, the world is seriously implementing plans on strengthening green technologies and the use of renewable energy sources as the means to address the ever-growing demands for energy worldwide. In recent years, numerous renewable energy technologies have been proposed, offering the ability to utilize low-grade heat and naturally replenish themselves at a rate that meets energy demands.

With promising features, the development of green technologies, such as thermoacoustics, shows great potential as a replacement for conventional refrigeration as they use inert gases as their working fluid rather than refrigerants (Luo et al. 2023). This is

primarily owing to the excellent qualities of dependability and environmental friendliness, which allow the inert gas to deliver worldwide energy services while leaving a tiny carbon footprint (Bhatti et al. 2023). According to Timmer et al. (2018), the effective operation of thermoacoustic devices necessitates a thorough comprehension in flow dynamics, transient phenomena, and the conversion of acoustic waves into energy, as this expertise guarantees the sustainability of thermoacoustic effects. Another key requirement for effective thermoacoustic devices is reliance upon the oscillatory motion of the working fluid. In this state, the compressible fluid moves back and forth through the porous structures, creating thermodynamic cycles that generate energy based on thermoacoustic principles. Luo et al. (2023) have determined that this characteristic of the flow is ideal for both the refrigeration and the power production applications, as it facilitates the thermodynamic cycle for energy conversion.

A standing-wave thermoacoustic system typically consists of a resonator tube, a porous stack, an acoustic driver and two heat exchangers positioned at the hot and cold ends, as shown in Figure 1.1. Kajurek and Rusowic (2021) mentioned that the acoustic driver generates an acoustic wave that propagates through the gaseous phase, thereby facilitating heat transfer, compression, and expansion processes upon its interaction with the solid surface of the stack plates. This will eventually results in a temperature disparity between the two ends of the stack. This is the reason the stack is referred to as the "core" of a thermoacoustic system, as it is the location where all thermoacoustic processes, comprising of the expansion, the compression and heat transfer, take place (Almukhtar Allafi et al. 2021). Another appealing feature of this simple alternative refrigeration system is the use of